

Synthesis and Evaluation of Uniformly Sized Carbamazepine-Imprinted Microspheres and Nanospheres Prepared with Different Mole Ratios of Methacrylic Acid to Methyl Methacrylate for Analytical and Biomedical Applications

Mehdi Esfandyari-Manesh,¹ Mehran Javanbakht,^{1,2} Fatemeh Atyabi,³ Rassoul Dinarvand³

¹Department of Chemistry, Amirkabir University of Technology, Tehran, Iran

²Nano Science and Technology Research Center, Amirkabir University of Technology, Tehran, Iran

³Nanotechnology Research Center, Tehran University of Medical Sciences, Tehran, Iran

Received 17 April 2011; accepted 23 September 2011

DOI 10.1002/app.36288

Published online 17 January 2012 in Wiley Online Library (wileyonlinelibrary.com).

ABSTRACT: In this work, we initiated to study new synthetic conditions to obtain uniformly sized molecularly imprinted polymers (MIPs) in the micrometer to nanometer range, using carbamazepine (CBZ) as a model template. The MIPs were successfully prepared by precipitation polymerization using methacrylic acid (MAA) and methyl methacrylate (MMA) as functional monomers at different mole ratios. The effect of MAA-to-MMA mole ratios on the morphology, binding, recognition, and release behaviors of the final particles were studied, and the adjusting possibility of these properties was also obtained. The produced polymers were characterized by Fourier transform infrared spectroscopy and differential scanning calorimetry, and their morphology was precisely examined by scanning electron microscopy and photon correlation spectroscopy. We obtained very uniform imprinted nanospheres and microspheres with diameter in the range of 120 nm to 1.74 μm under various conditions. Among the MIP nanospheres and microspheres prepared,

the MIPs using MAA-to-MMA mole ratio of 1 : 2 showed nanospheres with the lower polydispersity index (0.004) and the highest selectivity factor (10.4), which is defined as the binding ratio of CBZ and oxcarbazepine as template analog. Results from binding experiments proved that MIPs exhibit specific affinity to CBZ in contrast to control polymers, and this performance was affected by pH and concentration of the loading solution. Moreover, release experiments showed the controlled release of CBZ in long-time period. The 50% of loaded CBZ was released from the imprinted nanospheres within the first 30 h, whereas another 50% was released in the following 160 h. The release kinetics of CBZ from the MIPs highly affected with the properties of particles. © 2012 Wiley Periodicals, Inc. *J Appl Polym Sci* 125: 1804–1813, 2012

Key words: molecular imprinting; uniformly sized nanospheres; functional monomers; carbamazepine recognition; controlled release

INTRODUCTION

Molecular imprinting is recognized as a powerful technique to synthesize polymer-type artificial receptors.^{1–3} This technology is attracting widespread attention because of its potential to deliver robust molecular recognition elements targeted toward any guest really present in any environment (e.g., drug enantiomers, hormones, toxins, pesticides, peptides, proteins, and nucleic acids in matrixes ranging from pure organic solvents to biological fluids). In molec-

ular imprinting, highly crosslinked polymers can be used to form three-dimensional cavities with binding sites, mimicking the specificity of biologic molecules, through a course in which functional monomers and crosslinkers are copolymerized in the presence of the selected analyte as template. Molecularly imprinted polymers (MIPs) are often referred to as “artificial antibodies”. Unlike antibodies, MIPs are stable to extremes of pH, organic solvents, and temperature, which allows for more flexibility in the analytical methods.⁴

MIPs with well-controlled physical forms in different size ranges are highly desirable. For example, MIP nanospheres are very suitable to be used to develop binding assays, microfluidic separations, the stationary phase design for open-tubular capillary electrochromatography, and drug delivery systems.^{5,6} The MIP nanospheres are ideal to apply in the well-established nonseparation assay formats, for example, using measurements based on fluorescence

Correspondence to: M. Javanbakht (mehranjavanbakht@gmail.com).

Contract grant sponsors: Amirkabir University of Technology (Tehran, Iran), Nanotechnology Research Center of Tehran University of Medical Sciences (Tehran, Iran).

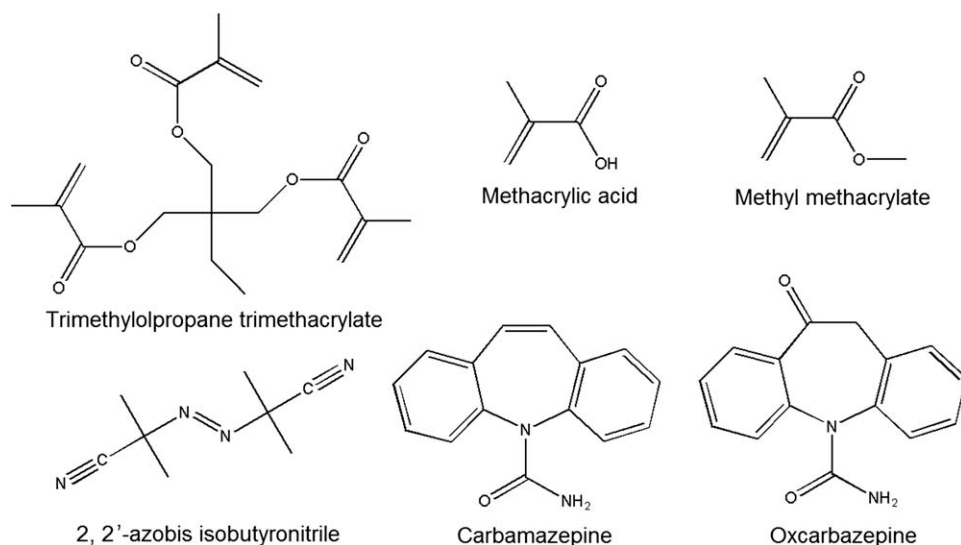


Figure 1 Structures of chemicals used in the molecular imprinting syntheses and the binding experiments.

polarization–depolarization or fluorescence resonance energy transfer technique.⁷ Nanosphere drug delivery carriers are able to protect drugs from degradation and improve the penetration or permeation of drugs across the mucosal surface.⁸

Conventionally, MIPs were synthesized by nonaqueous bulk polymerization techniques, which after grinding and sieving gave irregular particles with different sizes. Although this method allows easy preparation of large amount of MIPs, it is time consuming and yields only moderate amount of useful MIPs. The irregularity of size and shape of such MIP particles also made sample handling difficult, and chromatography efficiency reduced. For new analytical applications, the irregular particles are inferior to well-defined polymer beads, especially in developing MIP-based assays, sensor arrays, and separation modules. In addition to improving binding performance of MIPs, new physical formats of MIPs and more efficient synthetic methodologies were important research topics in the past years.^{9,10} Previously, uniformly sized MIPs for sulfamethazine,¹¹ clenbuterol,¹² (*S*)-ibuprofen,¹³ 17 β -estradiol,¹⁴ and (*S*)-propranolol¹⁵ have been prepared by a one-step, two-step, or multistep swelling and thermal polymerization methods. The polymerization methods available to prepare such monodispersed particles include water-based emulsions, seeded suspension polymerizations, nonaqueous dispersion polymerizations, and precipitation polymerizations. A relatively simple method for the preparation of imprinted polymers not requiring mechanical grinding or dispersion polymerization is precipitation polymerization, which yields uniformly sized nanospheres or microspheres.^{16–20}

Recently, we applied MIPs as synthetic artificial receptors in potentiometric detection of hydroxyzine²¹ and cetirizine²²; solid-phase extraction of verapamil,²³

metoclopramide,²⁴ and tramadol²⁵; and sustained release of dipyridamole^{26,27} and carbamazepine (CBZ).²⁸ The current study investigates the potential of precipitation polymerization as a promising technique for the synthesis of novel imprinted materials for various applications such as analytical field and drug delivery systems. In this work, we used the new synthetic conditions to obtain very uniformly sized imprinted nanospheres and microspheres for CBZ (Fig. 1) as a model template. CBZ is an anticonvulsant drug that is widely used in epilepsy treatment. Precipitation polymerization was carried out using methacrylic acid (MAA) and/or methyl methacrylate (MMA) as functional monomers, trimethylolpropane trimethacrylate (TRIM) as crosslinker, and 2,2'-azobis isobutyronitrile (AIBN) as initiator in acetonitrile as progenic solvent at 60°C. MAA, MMA, and TRIM (acrylate ester) that were the compounds of interest used in this work as the monomers are found to have biocompatibility and nontoxicity. Although poly(MAA)-, poly(MMA)-, and poly(acrylate ester)-based polymers are used for producing pharmaceutical products such as tablets and capsules,²⁹ MAA and *N*-vinylpyrrolidinone crosslinked by ethylene glycol dimethacrylate (TRIM analog crosslinker) are widely used as enteric polymers in the controlled delivery of paracetamol and aspirin.³⁰ The MAA-based nanospheres reported by Foss and Peppas³¹ had no cytotoxic side effects on the Caco-2 cell cultures.

The choice of functional monomer is more critical to the promotion of the imprinting efficiency and other properties of imprinted polymers.³² Normally, MIPs have been prepared with only a single type of functional monomer. Occasionally, combinations of functional monomers have been used to improve the properties and performance of MIPs with respect to those produced with a single functional

monomer.^{33,34} Acrylamide and 2-hydroxyethyl methacrylate (as neutral monomers), MAA and 4-vinylbenzoic acid (as acidic monomers), and 4-vinylpyridine (as basic monomer) were used as common functional monomers. To study and improve the morphology, binding, recognition, and release properties of MIPs when the ratio of the acidic monomer MAA and the neutral monomer MMA changed, several CBZ-imprinted polymers were prepared. The three-dimensional structure of binding sites in polymers containing MAA and MMA are improved because of steric hindrance of methyl groups in the side chains. The most successful noncovalent imprinting systems are based on MAA since the carboxylic acid groups of MAA serve as both hydrogen donor and acceptor. It is also a suitable functional monomer for CBZ, because carboxylic acid groups can form cyclic hydrogen bonds with the functional groups on CBZ (such as CONH₂ and CONR₂; Fig. 2). The neutral monomer of MMA was used to control composition and properties of MIPs.

Recently, the MIPs application in the drug release systems was reported. They can increase the residence time of the drug within the body by reducing the rate at which the drug is released.³⁵ Although its application in this field is just at an initial stage, the use of MIPs in the design of new drug delivery carriers and devices useful in closely related fields, such as diagnostic sensors or chemical traps to remove undesirable substances from the body, is receiving increasing attention.³⁶ In the current study, we present the first devices based on MIPs for controlled release of CBZ. The effect of functional monomer nature on the release behaviors of CBZ in sodium dodecyl sulfate (SDS) solution was studied to develop a material with controlled release properties for drug delivery applications. The binding properties of the MIPs to CBZ were evaluated by their binding capacity to CBZ in loading solution with different pH and concentrations. The molecular recognition ability with respect to template analog (oxcarbazepine [OCBZ]; Fig. 1) was also determined.

EXPERIMENTAL

Materials

MAA and MMA from Merck (Darmstadt, Hohenbrunn, Germany) were distilled in vacuum before use to remove the stabilizers. TRIM and AIBN were purchased from Sigma-Aldrich (Steinheim, Germany). AIBN was recrystallized from methanol before use. CBZ and OCBZ were obtained from the Ministry of Health and Medical Education (Tehran, Iran). SDS and acetonitrile were purchased from Merck. Dialysis tubes (Sigma dialyses tubes M_w cut-off 12 kDa, Steinheim, Germany) were heated in so-

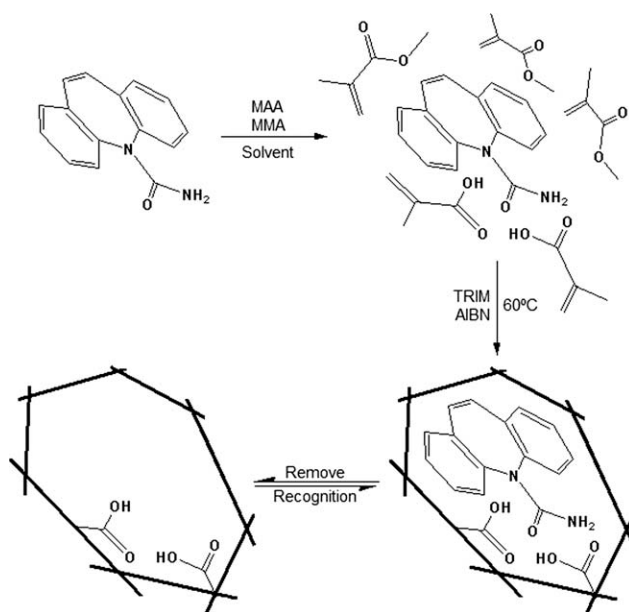


Figure 2 Schematic representation of the MIP synthesis and recognition.

dium bicarbonate (2 wt %)/ethylene diamine tetra acetic (0.05 wt %) solution and then kept under refrigeration in 0.05 wt % solution of sodium azide until use. Other reagents and solvents of an analytical reagent grade were used without further purification.

Apparatus

Scanning electron microscopy (SEM; PhilipsXL30 scanning microscope, Philips, Eindhoven, Netherlands) was used to determine the shape and surface morphology of the produced polymer particles. The particle size and size distribution of the particles were measured by photon correlation spectroscopy (PCS; Malvern Zetasizer ZS, Malvern, Worcestershire, UK). Polymer particles (2 mg) were mixed with acetonitrile (1 mL) sonicated in a bench-top ultrasonic cleaner (Tecno-Gaz, Tecna 6, Bologna, Italy) for 20 min until no particle aggregate could be observed. The colloidal sample was diluted with acetonitrile to a final concentration of 20 $\mu\text{g L}^{-1}$ prior to particle size measurement. The hydrodynamic size of the polymer particles was measured in acetonitrile at 25°C. The pH of solutions was adjusted using a Mettler Toledo pH meter (Seven Multi, Schwerzenbach, Switzerland) equipped with a combined glass-calomel electrode. Concentrations of solutions were analyzed by UV spectrophotometer (Scinco S-3100, Seoul, Korea). Particles were collected by centrifugation (Sigma 3K30, Ostrode am Harz, Germany). FTIR spectra (4000–400 cm^{-1}) in KBr were recorded on a Nicolet spectrometer (Magna IR 550, Madison, USA) using KBr pellets. Thermal

properties were investigated by a Mettler DSC 823 (Mettler Toledo, GmbH, Greifensee, Switzerland) equipped with a Julabo thermocryostat model FT100Y (Julabo Labortechnik GmbH, Germany). A Mettler Star software system (version 9.x) was used for the data acquisition. Indium was used to calibrate the instrument. The samples were scanned with a heating rate of $10^{\circ}\text{C min}^{-1}$ in $20\text{--}470^{\circ}\text{C}$ temperature range.

MIP and NIP preparation with precipitation polymerization

Molecularly imprinted nanospheres and microspheres were synthesized using precipitation polymerization under the conditions illustrated in Table I. For the preparation of the CBZ-imprinted polymer, the template (CBZ, 0.84 mmol) was dissolved in 5 mL of acetonitrile in a 50-mL thickwalled glass vessel, and then the functional monomers (MAA and/or MMA) were added. The mixture was homogeneously dispersed by sonication for 6 min. The solution was allowed to stir continuously for 90 min and the initiator (AIBN), the crosslinker (TRIM), and 35 mL of acetonitrile were added to the above solution and the mixture was homogeneously dispersed by sonication for 6 min. The solution was purged with a gentle flow of nitrogen for 5 min and sealed under nitrogen. The reaction vessel was inserted in a shaker bath and shaken horizontally at 50 cycles per minute. The temperature was ramped from 25 to 60°C within 40 min, thereafter kept for 20 h. After the polymerization, the polymer particles were separated by centrifuging at 17,000 rpm for 30 min. To remove template from the polymer matrix, the unleached imprinted polymers were washed with 40 mL of methanol containing 10% acetic acid (v/v) for five times for 1 h, until no template could be detected from the washing solvent by spectrometric method (at $\lambda = 285\text{ nm}$). The polymer particles were finally washed with same volume of deionized water and acetone, and the resulted leached imprinted polymers were dried at 50°C overnight. To verify that retention of template was due to molecular recognition and not due to nonspecific binding, a control, nonmolecularly imprinted polymer (NIP), was prepared as the same procedure, but with the omission of CBZ.

Binding experiments

The 40 mg of imprinted and nonimprinted particles were added to 6 mL of $85\ \mu\text{mol L}^{-1}$ CBZ water/acetonitrile (4 : 1, v/v) solution (pH = 7). A concentration of $85\ \mu\text{mol L}^{-1}$ CBZ was chosen in order to investigate the performance of MIPs in possible biomedical or biological applications. After the samples were stirred for 2 h, the polymer particles were cen-

TABLE I
Preparation of CBZ-Imprinted and Nonimprinted Polymers

Polymer	Template (mmol)	MAA (mmol)	MMA (mmol)	TRIM (mmol)
MIP1	0.84	2.52	–	1.68
NIP1	–	2.52	–	1.68
MIP2	0.84	1.68	0.84	1.68
NIP2	–	1.68	0.84	1.68
MIP3	0.84	0.84	1.68	1.68
NIP3	–	0.84	1.68	1.68
MIP4	0.84	–	2.52	1.68
NIP4	–	–	2.52	1.68

trifuged at 20,000 rpm for 30 min. The concentration of free CBZ in supernatant was measured by UV spectrophotometer. The amount of CBZ bound to the polymer particles was calculated by subtracting the amount of free CBZ from the CBZ initially added.

For determination of binding in solutions with different concentrations, 40 mg of MIP2 and NIP2 nanospheres were added to 6 mL of water/acetonitrile (4 : 1, v/v) solutions (pH = 7) of CBZ with specific initial concentrations ranging from 40 to $160\ \mu\text{mol L}^{-1}$. After the samples were stirred for 2 h, the amount of CBZ bound to the polymer particles was measured.

The effect of pH on the binding efficiency of CBZ was investigated by varying the pH of solutions from 3 to 11. All pH were adjusted with hydrochloric acid and sodium hydroxide solutions. Several batch experiments were performed by incubating 40 mg of MIP1 or NIP1 nanospheres with 6 mL of $85\ \mu\text{mol L}^{-1}$ of CBZ water/acetonitrile (4 : 1, v/v) and applying a gentle mixing under the desired range of pH for 2 h. Then, the amount of CBZ bound to the nanospheres was measured.

The selectivity of MIPs were determined by incubating 40 mg of imprinted polymers with 6 mL of $85\ \mu\text{mol L}^{-1}$ OCBZ (analog template) water/acetonitrile (4 : 1, v/v) solution (pH = 7), and then proceeding as for binding experiments.

In vitro drug release

Drug release from CBZ-loaded MIPs was carried out using dissolution method in SDS (1 wt %) aqueous solution as medium. The good solubility of CBZ in SDS (1 wt %) aqueous solution was used to maintain sink conditions.³⁷ The polymer particles (50 mg) were incubated with 6 mL of $1.0\ \text{mmol L}^{-1}$ CBZ water/acetonitrile (1 : 6, v/v) solution (pH = 7) for 1 h. Unbound CBZ was separated from the polymer particles by centrifugation at 20,000 rpm for 30 min. The amount of unbound CBZ by each polymer was determined by UV spectrophotometer. The

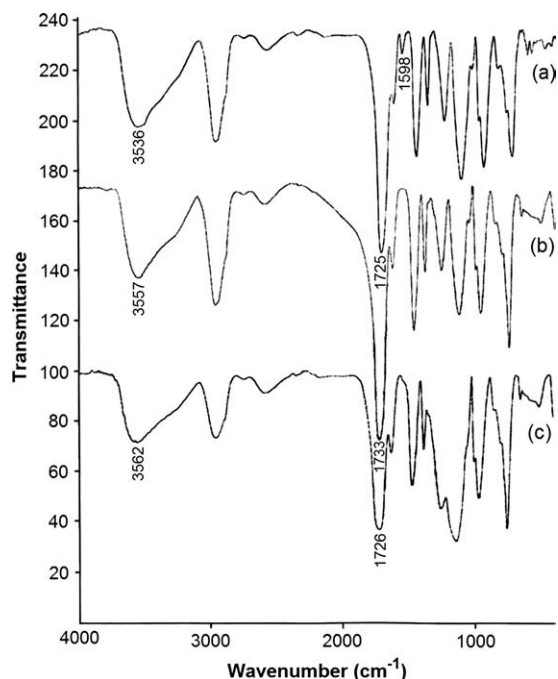


Figure 3 FTIR spectra of unleached MIP1 (a), leached MIP1 (b), and NIP1 (c).

centrifuged particles were suspended in 2 mL of SDS (1 wt %) aqueous solution and placed in a dialysis tube, then sealed at both ends with medicell clips, and soaked at 50 mL of SDS (1 wt %) aqueous solution. The medium was stirred at 100 rpm. Aliquots of 2 mL were withdrawn from the medium at designed time intervals. An equivalent volume of SDS (1 wt %) aqueous solution was added to maintain the volume of the medium at 50 mL. The amount of CBZ released from the polymer particles was quantified by UV analysis.

RESULTS AND DISCUSSION

Characterization

The infrared spectra of the nonimprinted polymer and unleached and leached imprinted polymer are shown in Figure 3. As a result of the hydrogen bonding with the $-\text{COOH}$ group of MAA, the $\text{C}=\text{O}$ stretching and the $\text{O}-\text{H}$ stretching at 1733 and 3557 cm^{-1} in the leached MIP were shifted to 1725 and 3536 cm^{-1} in the corresponding unleached MIP, respectively. Furthermore, there was another distinct difference between the FTIR spectra of the leached and unleached MIPs. In the unleached MIP, there was a sharp band with low relative intensity at 1598 cm^{-1} that disappeared in the corresponding leached MIP. This peak is related to the $\text{N}-\text{H}$ bending vibration of CBZ in the unleached MIP. Other absorption peaks match both those of MIP as well as NIP: 973 cm^{-1} (out-of-plane bending vibration of vinylic

$\text{C}-\text{H}$ bonds), 1147–1270 cm^{-1} (symmetric and asymmetric stretching vibration of ester $\text{C}-\text{O}$ bonds), 1388 cm^{-1} (bending vibration of $-\text{CH}_3$ groups), 1475 cm^{-1} (bending vibration of $-\text{CH}_2$ groups), 1634 cm^{-1} (stretching vibration of residual vinylic $\text{C}=\text{C}$ bonds), and 2965 cm^{-1} (stretching vibration of $\text{C}-\text{H}$ bonds).

Figure 4 depicts the differential scanning calorimetric results of the NIP1 and unleached and leached MIP1 nanospheres. DSC plots show that all polymers were thermally stable up to $\sim 250^\circ\text{C}$. At this temperature, the complex processes of decomposition were started. DSC plots with similar characteristics were obtained for leached MIP1 and NIP1. When compared with the unleached and leached MIP1, the endothermic transition at about 190°C was due to the melting of CBZ loaded on the unleached MIP1.

Morphologic analysis and size distribution of CBZ-imprinted nanospheres and microspheres

To study the size distribution of CBZ-imprinted polymer nanospheres and microspheres in solution, MIPs and NIPs were resuspended in acetonitrile and characterized with PCS. The PCS measurements provided valuable information about the hydrodynamic radius of the colloidal particles. Four samples of MIP nanospheres and microspheres with different composition were prepared. In these polymer samples, the crosslinker/functional monomer/template ratio was kept constant, whereas the MAA-to-MMA ratio was changed. Table II shows the different size distribution of imprinted and nonimprinted nanospheres and microspheres. By using neat acetonitrile as solvent, we obtained very uniform-sized nanospheres and microspheres with diameter in the range of 120 nm to 1.74 μm . Depending on the

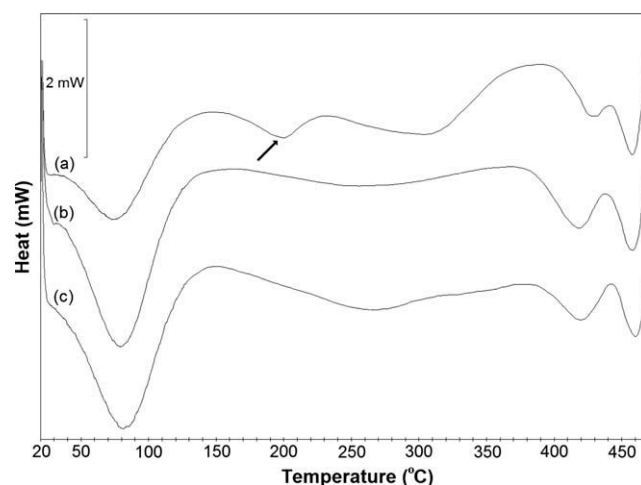


Figure 4 DSC thermograms of unleached MIP1 (a), leached MIP1 (b), and NIP1 (c).

TABLE II
Size Distribution of MIP and NIP Nanospheres and
Microspheres

Polymer	Average diameter (nm)	Polydispersity index
MIP1	174	0.022
NIP1	138	0.076
MIP2	129	0.017
NIP2	127	0.071
MIP3	152	0.004
NIP3	120	0.039
MIP4	1,742 ^a	–
NIP4	1,158 ^a	–

^a Average diameter measured by SEM.

monomers used, the CBZ-imprinted polymer nanospheres and microspheres had drastically different sizes. The use of MMA resulted in large particles (1.74 μm), whereas MAA gave uniformly sized nanospheres (174 nm). The results showed that the poly(MAA-co-TRIM) and the poly(MAA-co-MMA-co-TRIM) particles were uniform nanospheres, whereas the poly(MMA-co-TRIM) particles were nonuniform microspheres. The stability of polymer particles in the precipitation polymerization reaction is due to electrostatic charges and electrostatic repulsion.³⁸ The electrostatic charges are resulted in the presence of side groups on the polymer chains. The electrostatic charges of the polymer particles containing MAA are due to carboxylic acid side groups. The electrostatic charges cause the stability of growing polymer nuclei during the polymerization, and therefore, as a result, the number of resulting polymer particles would be increased and the size of them would be decreased.

The SEM images show spherical nanometer and micrometer particles (Fig. 5). There are no considerable differences in the morphology of imprinted and nonimprinted nanospheres and microspheres. The little difference in size and polydispersity index (index of the dimensional homogeneity of particles) of imprinted and nonimprinted polymers is due to the influence of template compound on the particle growth during the precipitation polymerization.¹⁶ In the absence of CBZ, functional monomer can form hydrogen-bonded dimers in the nonimprinting system, and the prepolymerization solution contains both functional monomer dimers and free functional monomer. In the imprinting system, there are additional molecular interactions between functional monomer and CBZ, which might somehow affect the growth of the crosslinked polymer nuclei. The SEM images of imprinted polymers containing MAA clearly show very spherical particles in the range of 129–174 nm. MIP2 containing MAA-to-MMA at mole ratio of 2 : 1 had a smaller average mean diameter (129 nm). The results obtained by PCS tests were higher than those observed by SEM that was related

to swelling of polymer nanospheres in investigated solvent. Figure 6 shows the size distribution for MIP3 and NIP3 nanospheres that are corresponding with the SEM images in Figure 5(e,f). The SEM images excellently show the well-defined spherical nanoparticles in narrow size distribution. MIP3 with the MAA-to-MMA mole ratio of 1 : 2 had a lower polydispersity index of 0.004. We should point out that the SEM and the PCS results suggest that the nanospheres containing MAA had a very narrow particle size distribution that is a highly desirable characteristic in many applications such as solid-phase microextraction, chemical sensors, capillary electrochromatography, and biomedical applications.¹⁶

CBZ binding to molecularly imprinted nanospheres and microspheres in water/acetonitrile solution

Specific binding provided by the imprinted sites can be estimated by measuring the difference of CBZ uptake between the imprinted and nonimprinted nanospheres and microspheres. The results from binding experiments showed that all imprinted polymers had much higher CBZ binding than corresponding nonimprinted polymers. When MAA was used as the functional monomer, the imprinted nanospheres and microspheres displayed higher CBZ binding (Table III); this amount was increased from 21.6% for MIP4 (MAA-to-MMA, 0 : 3) to 46.8% for MIP1 (MAA-to-MMA, 3 : 0). This phenomenon was most probably due to the fact that the carboxylic acid groups of MAA had additional interactions with the functional groups of CBZ. The specific binding was reduced with decrease of MAA percentage in the polymers. The specific binding recovery of CBZ at MAA-to-MMA mole ratios of 3 : 0, 2 : 1, 1 : 2, and 0 : 3 were 13.2%, 15.2%, 9.3%, and 3.5%, respectively. The optimum functional monomers ratio for the specific binding of CBZ in water/acetonitrile solution (4 : 1, v/v) was 2 : 1 (MIP2). The excess amount of MAA in MIP1 when compared with MIP2 reduced the imprinting efficiency of MIP1.

The CBZ binding of MIP2 and NIP2 in loading solutions with different concentrations of 40, 80, 120, and 160 $\mu\text{mol L}^{-1}$ was determined. MIP2 bound about 0.49, 1.22, 1.93, and 2.75 mg of CBZ per 1 g of polymer in different concentrations, respectively. The amount of CBZ binding and the binding difference of imprinted and nonimprinted polymers were increased gradually with the increase of the CBZ concentration in the loading solution. The binding difference between MIP2 and NIP2 were obtained 0.19, 0.45, 0.45, and 0.87 mg of CBZ per 1 g of polymer, respectively. This kind of binding kinetic of imprinted polymers is similar to that of biological receptors.

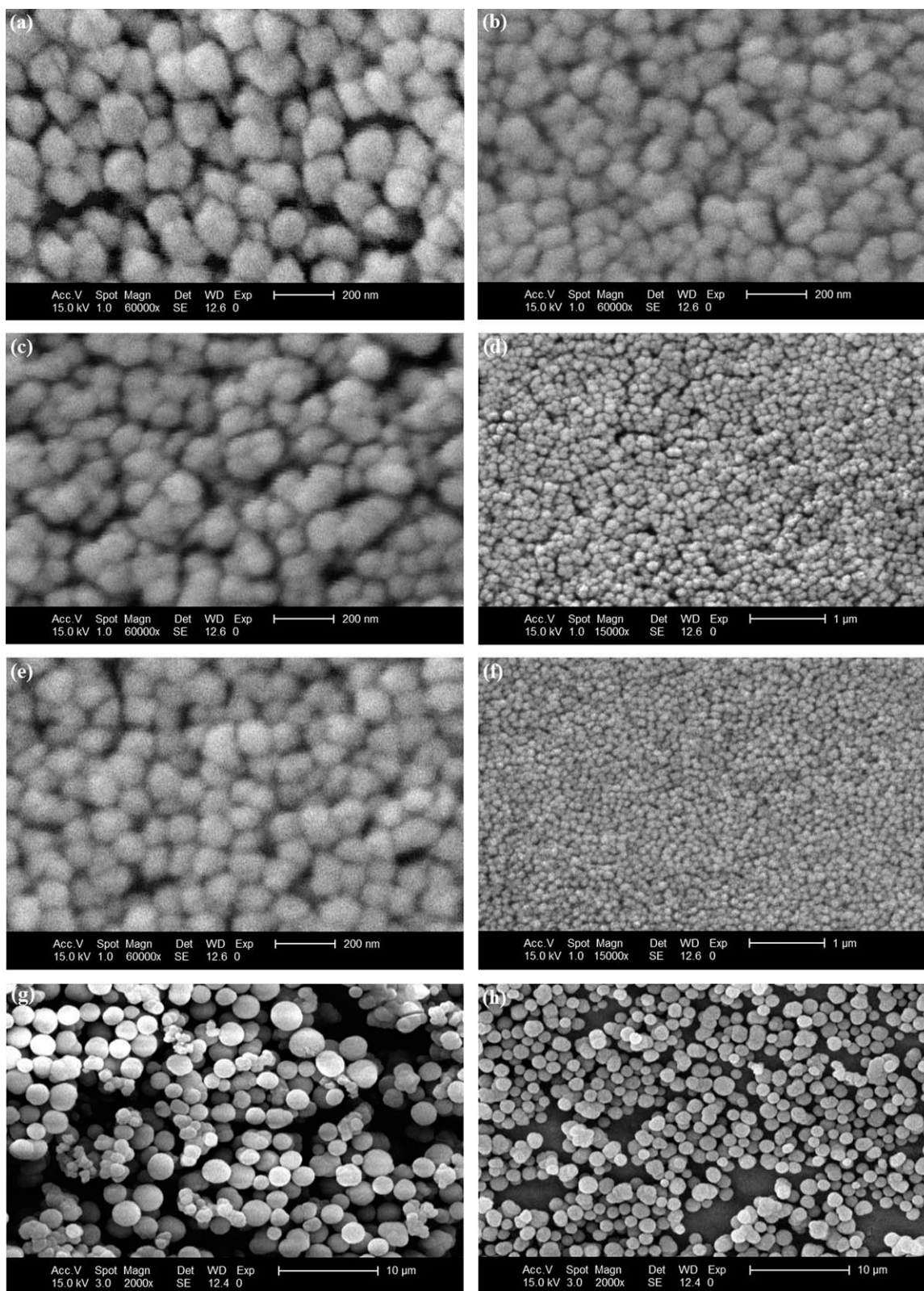


Figure 5 Scanning electron micrographs of MIP1 (a), NIP1 (b), MIP2 (c and d), MIP3 (e and f), MIP4 (g), and NIP4 (h).

The effect of pH on the binding of imprinted and nonimprinted polymers is shown in Figure 7. There was a trend of the increase binding with the increase of pH up to 7.0; the maximum binding was

observed at pH 7.0, and at higher pH (>7.0), the binding of CBZ was decreased. These results can be explained as follows: the polymer nanospheres with the carboxylic acid group of MAA bound the

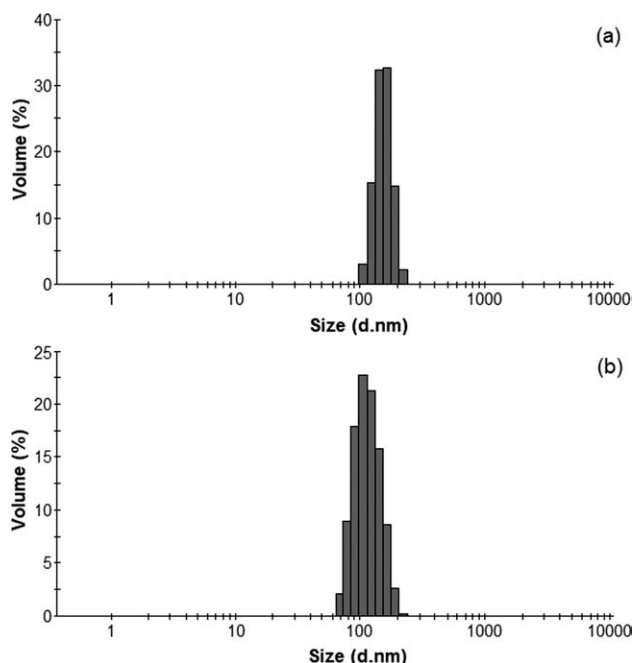


Figure 6 Particle size distribution of MIP3 (a) and NIP3 (b) measured by photon correlation spectroscopy.

template molecule by ionic and hydrogen bonding interaction. At pH 13 or below, which was lower than the pK_a values of CBZ (13.4), the solute of CBZ was completely protonated. At acidic or basic conditions, the acidity and basicity of the medium was so strong that its interaction with the template molecule exceeded the imprinting effect. In addition, at higher pH, the negative charge of the polymer was increased, mainly as carboxylic acid groups were deprotonated. At neutral pH, the best conditions existed for the formation of the hydrogen bonding between functional groups of binding sites and template molecules.

Selectivity of CBZ-imprinted nanospheres and microspheres

OCBZ as structural analog of CBZ was selected to investigate the selectivity of the MIP particles. The molecular recognition abilities of CBZ-imprinted polymers toward template analog were evaluated using the selectivity factor (α) as ratio between template and template analog binding³⁹:

TABLE III
Amount of CBZ Bound by MIP and NIP Nanospheres and Microspheres

Polymer	CBZ bound by MIP (%)	CBZ bound by NIP (%)
1	46.8	33.6
2	40.5	25.3
3	33.9	24.6
4	21.6	18.1

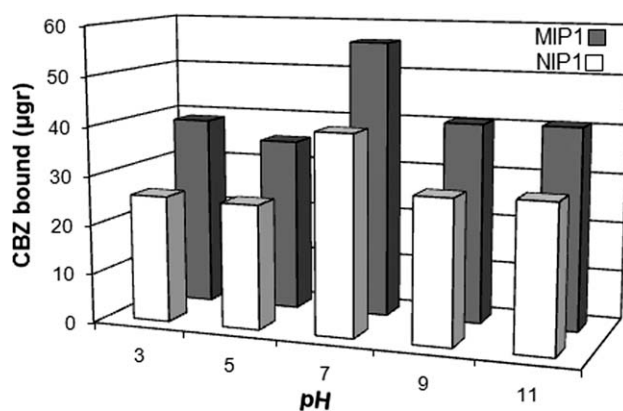


Figure 7 CBZ binding of MIP1 and NIP1 nanospheres in loading solution with different pHs.

$$\alpha_{\text{template}/\text{analog}} = \frac{\text{template bound}}{\text{analog bound}}$$

Table IV shows the OCBZ binding and selectivity factors of CBZ-imprinted polymers. OCBZ binding to CBZ-imprinted polymer is as a result of the non-selective and nonspecific binding. OCBZ binding to MIPs containing MAA increased with the increase of MAA percentage. The highest selectivity factor of 10.3 was obtained for MIP3 (MAA-to-MMA, 1 : 2). In this mole ratio, good cavities for imprinting of CBZ were obtained. In contrast, the MIP1 and MIP4 gave little selectivity factors of 2.1 and 2.5 for CBZ, respectively. These values were low, because MIP1 had excess amount of MAA (led to decrease of imprinting efficiency and increase of nonspecific binding), and MIP4 had no MAA as an appropriate functional monomer for interaction with CBZ.

Drug release studies

In vitro release behaviors of CBZ from the MIP nanospheres and microspheres were studied in SDS (1 wt %) media. Figure 8 shows the percent release of CBZ from MIPs against incubation time. The quick first release of CBZ is to be ascribed to weakly adsorbed and available molecules, while in the longer time period, the CBZ molecules more tightly bound to the polymer networks are released. Many manufacturing parameters determine the drug release behavior from MIP nanospheres and microspheres. The

TABLE IV
Selectivity Properties of CBZ-Imprinted Polymers

Polymer	OCBZ bound (%)	$\alpha_{\text{template}/\text{analog}}$
MIP1	22.4	2.1
MIP2	7.4	5.5
MIP3	3.3	10.3
MIP4	8.7	2.5

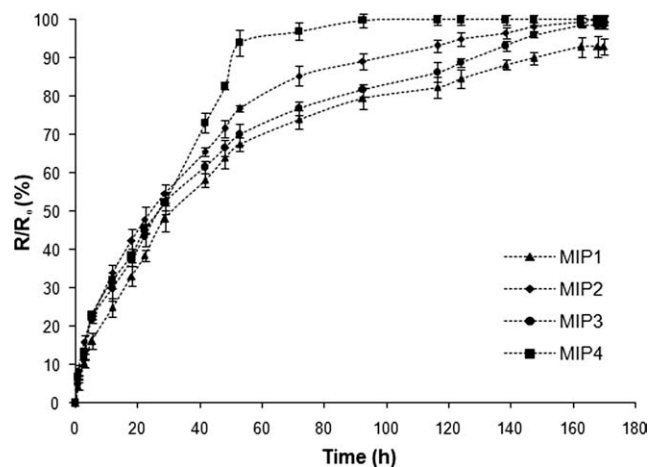


Figure 8 Release of CBZ in sodium dodecyl sulfate solution (1 wt %) by imprinted polymers. R/R_0 is the ratio of the amounts of CBZ released with respect to the initial amount in the imprinted polymers. The data are presented as mean \pm SD ($n = 3$).

release of CBZ from MIP4 was faster than other ones, and 87% of the loaded CBZ was released in 50 h. The fast release would be interpreted as weak interactions between the CBZ and binding points of polymer networks because of the absence of MAA. MIP1, MIP2, and MIP3 released about 65, 73.5, and 68.5% of CBZ in 50 h. MIP1 nanospheres, having maximum percentage of MAA, showed slower rate and released about 90% of CBZ in 7 days. However, MIP2 showed faster release than MIP3; this phenomenon was due to the higher hydrophilicity and smaller size of MIP2 nanospheres. The higher percentage of MAA in MIP2 than MIP3 increased the hydrophilicity of MIP2. The small size of MIP2 nanospheres increased the solid-liquid contact of polymer particles to solution and, therefore, increased the rate of CBZ release.

Imprinted polymers are introduced as drug delivery carriers because they act as a drug reservoir due to their crosslinked network. These polymers can increase the presence time of the drug in the body by decreasing the release rate. They can also keep the drug concentration below the concentration where toxic effects become dominant.

CONCLUSION

The wide range of commercial applications for nanospheres and microspheres has encouraged much recent research in this field. In summary, very uniformly sized CBZ-imprinted nanospheres and microspheres with different ratios of MAA versus MMA were carefully studied as for its morphology, release profiles, affinity, and selectivity to CBZ and the analog OCBZ by the methods including SEM, PCS,

equilibrium experiments, and UV spectroscopy. The change of particles size was achieved by varying the ratio of two different functional monomers, basically in the same precipitation polymerization system. The presence of MAA in polymerization reaction resulted in the preparation of the monodispersed polymer particles in nanoscale. Among the MIP nanospheres and microspheres prepared, the MIPs using MAA-to-MMA mole ratio of 1 : 2 showed high uniformly sized nanospheres with the lower polydispersity index (0.004). The imprinted polymers prepared by 1 : 2 and 2 : 1 mole ratios of MAA-to-MMA showed best imprinting efficiency and had high selectivity and specific binding, respectively. The increase in release rate was observed at greater amounts of MMA, which is related to the decrease in interaction intensity between the CBZ molecules and binding points of polymer. By using imprinted polymers containing different mole ratios of MAA and MMA, the controlled release of CBZ was obtained. The combined use of two different functional monomers in precipitation polymerization opened new possibilities of fine adjusting properties (morphology, molecular recognition, and release properties) of MIPs in other systems such as analytical and bioanalytical applications.

References

- Mosbach, K. *Trends Biochem Sci* 1994, 19, 9.
- Haupt, K.; Mosbach, K. *Chem Rev* 2000, 100, 2495.
- Ye, L.; Mosbach, K. *React Funct Polym* 2001, 48, 149.
- Tokonami, S.; Shiigi, H.; Nagaoka, T. *Anal Chim Acta* 2009, 641, 7.
- Ye, L.; Surugiu, I.; Haupt, K. *Anal Chem* 2002, 74, 959.
- De Boer, T.; Mol, R.; De Zeeuw, R. A.; De Jong, G. J.; Sherrington, D. C.; Cormack, P. A. G.; Ensing, K. *Electrophoresis* 2002, 23, 1296.
- Hunt, C. E.; Pasetto, P.; Ansell, R. J.; Haupt, K. *Chem Commun* 2006, 16, 1754.
- Atyabi, F.; Aghaei Moghaddam, F.; Dinarvand, R.; Zohuriaan-Mehr, M. J.; Ponchel, G. *Carbohydr Polym* 2008, 74, 59.
- Ko, D. Y.; Lee, H. J.; Jeong, B. *Macromol Rapid Commun* 2006, 27, 1367.
- Vaihinger, D.; Landfester, K.; Krauter, I.; Brunner, H.; Tovar, G. E. M. *Macromol Chem Phys* 2002, 203, 1965.
- Chen, Z.; Zhao, R.; Shangquan, D.; Liu, G. *Biomed Chromatogr* 2005, 19, 533.
- Masci, G.; Aulenta, F.; Crescenzi, V. *J Appl Polym Sci* 2002, 83, 2660.
- Haginaka, J.; Sanbe, H.; Takehira, H. *J Chromatogr A* 1999, 857, 117.
- Piscopo, L.; Prandi, C.; Coppa, M.; Sparnacci, K.; Laus, M.; Lagana, A.; Curini, R.; D'Ascenzo, G. *Macromol Chem Phys* 2002, 203, 1532.
- Haginaka, J.; Sakai, Y. *J Pharm Biomed Anal* 2000, 22, 899.
- Yoshimatsu, K.; Reimhult, K.; Krozer, A.; Mosbach, K.; Sode, K.; Ye, L. *Anal Chim Acta* 2007, 584, 112.
- Lai, J.; Yang, M.; Niessner, R.; Knopp, D. *Anal Bioanal Chem* 2007, 389, 405.
- Chaitidou, S.; Kotrotsiou, O.; Kotti, K.; Kammona, O.; Bukhari, M.; Kiparissides, C. *Mater Sci Eng B* 2008, 152, 55.

19. Sanbe, H.; Haginaka, J. *J Pharm Biomed Anal* 2002, 30, 1835.
20. Downey, J. S.; Frank, R. S.; Li, W. H.; Stover, H. D. *Macromolecules* 1999, 32, 2838.
21. Javanbakht, M.; Eynollahi Fard, S.; Mohammadi, A.; Abdouss, M.; Ganjali, M. R.; Norouzi, P.; Safaraliee, L. *Anal Chim Acta* 2008, 612, 65.
22. Javanbakht, M.; Eynollahi Fard, S.; Abdouss, M.; Mohammadi, A.; Ganjali, M. R.; Norouzi, P.; Safaraliee, L. *Electroanalysis* 2008, 20, 2023.
23. Javanbakht, M.; Shaabani, N.; Mohammadi, A.; Abdouss, M.; Ganjali, M. R.; Norouzi, P. *Curr Pharm Anal* 2009, 5, 269.
24. Javanbakht, M.; Shaabani, N.; Akbari-Adergani, B. *J Chromatogr B* 2009, 877, 2537.
25. Javanbakht, M.; Attaran, A. M.; Namjumanesh, M. H.; Esfandyari-Manesh, M.; Akbari-Adergani, B. *J Chromatogr B* 2010, 878, 1700.
26. Esfandyari-Manesh, M.; Javanbakht, M.; Atyabi, F.; Mohammadi, A.; Mohammadi, S.; Akbari-Adergani, B.; Dinarvand, R. *Mater Sci Eng C*, 2011, 31, 1692.
27. Javanbakht, M.; Mohammadi, S.; Esfandyari-Manesh, M.; Abdouss, M. *J Appl Polym Sci* 2011, 119, 1586.
28. Esfandyari-Manesh, M.; Javanbakht, M.; Atyabi, F.; Badiei, A.; Dinarvand, R. *J Appl Polym Sci* 2011, 121, 1118.
29. Jantararat, C.; Tangthong, N.; Songkro, S.; Martin, G. P.; Suedee, R. *Int J Pharm* 2008, 349, 212.
30. Devine, D. M.; Devery, S. M.; Lyons, L. G.; Geever, L. M.; Kennedy, J. E.; Higginbotham, C. L. *Int J Pharm* 2006, 326, 50.
31. Foss, A. C.; Peppas, N. A. *Eur J Pharm Biopharm* 2004, 57, 447.
32. Wu, X.; Goswami, K.; Shimizu, K. D. *J Mol Recognit* 2008, 21, 410.
33. Feás, X.; Fente, C. A.; Hosseini, S. V.; Seijas, J. A.; Vázquez, B. I.; Franco, C. M.; Cepeda, A. *Mater Sci Eng C* 2009, 29, 398.
34. Wang, P.; Hu, W.; Su, W. *Anal Chim Acta* 2008, 615, 54.
35. Cunliffe, D.; Kirby, A.; Alexander, C. *Adv Drug Delivery Rev* 2005, 57, 836.
36. Alvarez-Lorenzo, C.; Concheiro, A. *J Chromatogr B* 2004, 804, 231.
37. Katzhendler, I.; Azoury, R.; Friedman, M. *J Controlled Release* 2000, 65, 331.
38. Pich, A.; Richtering, W. *Advances in Polymer Science*; Springer: Berlin, 2010.
39. Silvestri, D.; Borrelli, C.; Giusti, P.; Cristallini, C.; Ciardelli, G. *Anal Chim Acta* 2005, 542, 3.